HHS Public Access

Author manuscript

Acta Biomater. Author manuscript; available in PMC 2021 September 01.

Published in final edited form as:

Acta Biomater. 2020 September 01; 113: 501–511. doi:10.1016/j.actbio.2020.06.019.

Enzyme-Responsive Polymeric Micelles of Cabazitaxel for Prostate Cancer Targeted Therapy

Ashutosh Barve, **Akshay Jain**, **Hao Liu**, **Zhen Zhao**, **Kun Cheng**[*]

Division of Pharmacology and Pharmaceutical Sciences, School of Pharmacy, University of Missouri-Kansas City, 2464 Charlotte Street, Kansas City, MO 64108

Abstract

Cabazitaxel, a novel tubulin inhibitor with poor affinity for P-glycoprotein, is a second-generation taxane holding great promise for the treatment of metastatic castration-resistant prostate cancer. However, its poor solubility and lack of target-ability limit its therapeutic applications. Herein, we develop a biodegradable, enzyme-responsive, and targeted polymeric micelle for cabazitaxel. The micelle is formed from two amphiphilic block copolymers. The first block copolymer consists of PEG, an enzyme-responsive peptide, and cholesterol; whereas the second block copolymer consists of a targeting ligand (DUPA), PEG and cholesterol. The enzyme-responsive peptide is cleavable in the presence of matrixmetaloproteinase-2 (MMP-2), which is overexpressed in the tumor microenvironment of prostate cancer. The micelle showed a very low critical micelle concentration (CMC), high drug loading, and high entrapment efficiency. Release of cabazitaxel from the micelle is dependent on the cleavage of the enzyme-responsive peptide. Moreover, the micelle showed dramatically higher cellular uptake in prostate cancer cells compared to free cabazitaxel. Importantly, the ligand-coupled polymeric micelle demonstrated better inhibition of tumor growth in mice bearing prostate cancer xenografts compared to unmodified micelle and free cabazitaxel. Taken together, these findings suggest that the enzyme-responsive cabazitaxel micelle is a potent and promising drug delivery system for advanced prostate cancer therapy.

Graphical Abstract

[*]Corresponding author: Kun Cheng, Ph.D., Professor, Division of Pharmacology and Pharmaceutical Sciences, School of Pharmacy, University of Missouri-Kansas City, 2464 Charlotte Street, Kansas City, MO 64108, Phone: (816) 235-2425, Fax: (816) 235-5779, chengkun@umkc.edu.

Declaration of interests

The authors declare that they have no known competing financial interests or personal relationships that could have appeared to influence the work reported in this paper.

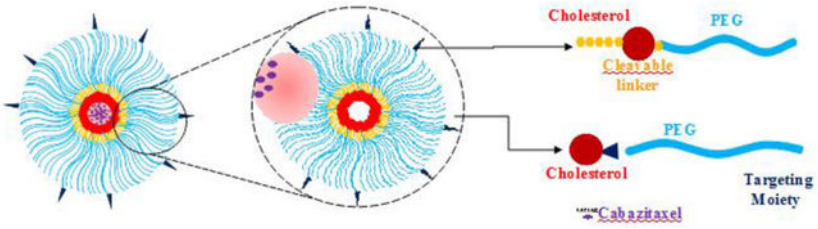

Keywords

Cabazitaxel; DUPA; Micelle; Cholesterol; Enzyme-Responsive; Prostate Cancer

1. Introduction

Despite advances in early screening and continuous research efforts, prostate cancer remains the most common cancer in the United States and accounts for almost 1 in 5 new cancer diagnoses. Prostate cancer is also the second leading cause of cancer death in American men, with an expected 31,620 deaths in 2019.[1] Current treatments for prostate cancer include surgery, radiation therapy, cryotherapy, hormone therapy, chemotherapy, and the Sipuleucel-T (Provenge) vaccine.[2, 3] Even in the age of immunotherapy with checkpoint inhibitors, chemotherapy is still the mainstay for advanced prostate cancer.

Cabazitaxel, a novel tubulin inhibitor with poor affinity for P-glycoprotein, is a second-generation taxane holding great promise for the treatment of metastatic castration-resistant prostate cancer. Cabazitaxel is a semisynthetic derivative of a natural toxoid and was approved in 2010 by the Food and Drug Administration (FDA) as the second line of treatment for metastatic castration-resistant prostate cancer. Notably, it is effective for the treatment of docetaxel-resistant cancers. However, the major limitations of cabazitaxel include the lack of specificity and very low water solubility.[4–6] Therefore, there is an urgent need to develop a targeted drug delivery system to deliver cabazitaxel specifically to tumor tissue and subsequently reduce the side effects.[7, 8]

Prostate-specific membrane antigen (PSMA) is a type II membrane glycoprotein protein with an extensive extracellular domain.[9] It is a well-established tumor antigen and is expressed in normal and malignant prostate cells, as well as other tissues. In particular, the levels of expression of PSMA in prostate cancer cells, especially in the advanced castration-resistant prostate cancer cells, are about a thousand-fold greater than that on normal tissues.[9] In addition, overexpression of PSMA is a predictive indicator for recurrence in primary prostate cancer.[10] Taken together, PSMA is a validated marker for targeted drug delivery to prostate cancer.[3, 11]

A variety of PSMA-specific ligands such as peptides, aptamers, antibodies, and ScFv have been employed to specifically deliver therapeutic agents to prostate cancer cells.[3, 11–17] Among them, 2-[3-(1,3-dicarboxypropyl)ureido]pentanedioic acid (DUPA) is a small molecule with a high affinity (K_i=8 nM, IC_{50}=47 nM) towards PSMA.[18, 19]DUPA was originally discovered as a substrate of PSMA but then adopted as a PSMA-targeting ligand

for anti-prostate cancer agents.[18–21]For example, Lutetium-177-labeled DUPA (^{177}Lu-PSMA-617) has moved to clinical trials in Europe as a radioligand therapy for patients with metastatic CRPC. ^{177}Lu-PSMA-617 showed good safety and higher efficacy than other third-line systemic therapies in metastatic CRPC patients.[21] Moreover, studies have shown that cytotoxic agents conjugated to DUPA and DUPA derivatives can effectively target PSMA overexpressing prostate cancer cells.[20]

Stimuli-responsive delivery systems have attracted increasing attention in tumor-targeted delivery. The tumor microenvironment has unique physiological characteristics such as hypoxia, acidic pH, and specific enzymes.[3, 22, 23] These endogenous stimuli provide great opportunities to trigger the release of therapeutic agents once they extravasate into the tumor microenvironment, leading to accelerated drug release at the target site and more efficient tumor penetration.[23, 24] Among these stimuli, tumor-specific enzymes, such as PSA and matrix metaloproteinase-2 (MMP-2), have been successfully used to deliver anti-cancer agents to various cancers.[24–30] MMP-2 is overexpressed in many types of cancers including prostate cancer.[31–33]

In this study, we develop a biocompatible polymeric micelle to encapsulate cabazitaxel. DUPA is coupled to the micelle to target PSMA on prostate cancer cells. The amphiphilic building block of the micelles is composed of cholesterol as the hydrophobic core and PEG as the hydrophilic outer shell. An MMP-2-responsive linker was incorporated in the amphiphilic building blocks to dissociate the micelle and release the payload in the tumor microenvironment of prostate cancer, leading to improved cellular uptake of cabazitaxel. The micelle shows a low critical micelle concentration (CMC), high drug loading, and high entrapment efficiency. The release of cabazitaxel from the micelle is dependent on the cleavage of the MMP-2-responsive peptide. The micelle exhibits higher cellular uptake in prostate cancer cells compared to free cabazitaxel. Most importantly, the polymeric micelle demonstrates better inhibition of tumor growth than free cabazitaxel in mice bearing prostate cancer xenografts.

2. Materials and Methods

2.1 Materials

Cabazitaxel and PEG-NHS were purchased from LC Laboratories (Woburn, MA). PEG_{3000}-Cholesterol was purchased from Biochempeg (Watertown, MA). Human recombinant MMP-2 protein was obtained from Millipore Sigma (Burlington, MA). α,γ-Di-*tert*-butyl glutamate, and triphosgene were purchased from Alfa Aesar(Haverhill, MA). N,N-Diisopropylethylamine (DIPEA), trifluoroacetic acid (TFA), triethylamine, triisopropylsilane (TIPS), HATU, HCTU, and piperidine were ordered from Fisher Scientific (Hampton, NH). Peptides were synthesized by United BioSystems (Herndon, VA). C4–2 cell line was purchased from the American Type Culture Collection (Rockville, MD).

2.2 Synthesis of DUPA (2-[3-(1,3- Bis-*tert*-butoxycarbonyl-propyl)-ureido]pentanedioic Acid-*tert*-Butyl Ester

DUPA was synthesized as reported.[20, 34, 35] Briefly, triethylamine (TEA, 8.19 mmol) was added into a solution of L-glutamate di-*tert*-butyl ester hydrochloride (3.39 mmol) and triphosgene (1.12 mmol) in DCM (25 mL), stirred at −78°C under nitrogen atmosphere for 2 h, and then mixed with the solution of L-Glu(OBn)-OtBu (3.72 mmol) and TEA (4.91 mmol) in DCM (5 mL). The reaction mixture was stirred at room temperature overnight, followed by adding 1 M HCl (1 mL) to quench the reaction. After washing with brine and drying over Na_2SO_4, the product 1 (432 mmol) was dissolved in DCM, and 10% Pd/C was added to deprotect the benzyl groups. The mixture was hydrogenated at room temperature for 24 h and washed with DCM. Finally, DUPA (2) was collected as a colorless oil and crystallized using hexane:DCM (1:1, v/v). The product was checked by TLC using hexane:EtOAc (40:60, v/v), and the retention factor is 0.58.(*m*/*z*): $(M + H)^+$ calculated for $C_{23}H_{41}N_2O_9$, 489.2912; found, 489.28.

2.3 Synthesis of Chol-PLGVRK-PEG_{2000}(4)

Chol-PLGVRK-PEG_{2000}(4) was synthesized by conjugating PEG-NHS to Chol-PLGVRK-NH_2.Chol-PLGVRK (1) was synthesized as previously reported with modifications.[36, 37] Briefly, PLGVRK on resin was suspended in 5 mL of ice-cold anhydrous DCM, followed by dropwise addition of 500 mg of cholesteryl chloroformate dissolved in 5 mL anhydrous DCM and incubation overnight under vigorous stirring on ice. The reaction mixture was washed 3 times with DCM, and the residual protecting groups in the peptide were removed by TFA. (*m*/*z*): (M + H)+ calculated for $C_{58}H_{101}N_{10}O_9$, 1081.82; found, 1081.50.

Next, PEG_{2000}-NHS was conjugated to chol-PLGVRK-NH_2 as reported with modifications. [37–39] Briefly,PEG_{2000}-NHS (0.1 mmol) and Chol-PLGVRK-NH2 (0.2 mmol) were separately dissolved in DCM (5 mL). The NHS group of the PEG reacted with the primary amine in the side chain of K (lysine), which was activated by DIPEA (0.2 mmol) in anhydrous DCM. The PEG_{2000}-NHS solution was added dropwise into the Chol-PLGVRK-NH2 solution, and the mixture was stirred for 24 h. The solvent was removed under vacuum, and the product Chol-PLGVRK-PEG_{2000} was purified by HPLC.

2.4 Synthesis of Chol-PEG_{3000}-DUPA (5)

Chol-PEG_{3000}-DUPA (5) was synthesized as previously reported with minor modification. [20, 40–42] Briefly, DUPA (0.1 mmol) was dissolved in dichloromethane (DCM), followed by the addition of EDC (0.2 mmol). After adding PEG_{3000}-Chol-NH2 (0.1 mmol) dissolved in DCM, the reaction mixture was stirred at room temperature for 24 h. The protecting groups of DUPA were removed by 50% TFA, and reaction mixture was continuously stirred for 12 h, dialyzed (MWCO of 1.0 kDa), and lyophilized to yield Chol-PEG_{3000}-DUPA (0.6 g, 28%).

2.5 Fabrication of Cabazitaxel-Loaded Polymeric Micelles

Cabazitaxel-loaded micelles were prepared using the solvent evaporation method as reported.[43] Briefly, the two block polymers were dissolved in a 1:9 molar ratio (block-1:block-2) in DCM, and the drug was separately dissolved in DCM. The polymer and

drug solutions were then mixed in a round bottom flask. The organic solvent was removed using a rotary evaporator at 37°C, and the resulting thin film was rehydrated with distilled deionized water. The micelles were sonicated for 5 min and filtered through a 0.22 μm membrane to remove un-encapsulated drug.[43]

2.6 Characterization of the Polymeric Micelle

Particle size and zeta potential of the micelle were measured using a Malven Zetasizer Nano-ZS(Malvern Instruments, MA).Morphology of the micelles was examined using a CM12 Transmission Electron Microscope (TEM) (Philips, Germany).Critical micelle concentration (CMC) of the polymeric micelle was determined using iodine as a probe.[43–45] A series of dilutions of the polymer ranging from 0.00005 to 4 mg/mL were prepared in DI water. The iodine solution was prepared by dissolving 0.05g iodine and 0.1 g potassium iodide in 15 mL DI water, and 25 μL of the solution were added to the polymer solutions. After incubation for 15h in dark at room temperature, 200 μL of this solution were transferred to a 96-well plate, and the absorbance was measured at 366 and 460nm. The CMC was calculated from the intersection of the two tangents drawn to the curve at high and low concentrations.[43, 44]

Drug loading capacity and encapsulation efficiency of the micelle were determined according to a previously reported method.[46] Briefly, micelles were prepared at different polymer:drug ratios (1:2, 1:1, 1:0.5, 1:0.25, 1:0.1, and 1:0.05, w/w) as described above. The lyophilized formulations were dissolved in DCM to dissociate the micellar structure, and the content of Cabazitaxel in the micelle was determined using HPLC with a C-18 reverse-phase column (4.6×250 mm, 5 μm).[24] Drug loading capacity and entrapment efficiency were calculated according to the following equations:

$$\text{Drug loading } (\%) = 100 \times \left(\frac{\text{Weight of drug in the micelle}}{\text{Weight of drug in the micelle + weight of polymer added}} \right)$$

$$\text{Drug entrapment } (\%) = \frac{\text{Weight of drug in the micelle}}{\text{Weight of drug added}}$$

2.7 Cleavage Study of the MMP-2-ResponsivePeptide

The MMP-2-responsive peptide PLGVRK (300 μM) was incubated with PBS or recombinant human MMP-2 proteinat 37 °C. Aliquots of 30 μL from each sample were collected at various time intervals (0, 3 and 6 h) and incubated with 90 μL of acetonitrile containing 0.1% TFA at room temperature for 5 min. The concentration of the intact peptide in the organic phase was determined using HPLC.

2.8 *In Vitro* Drug Release

In vitro drug release of the polymeric micelle was conducted in 0.5 M Tris buffer containing recombinant human MMP-2 protein (200ng/mL). The micelles were dispersed in 2 mL of the solution in a dialysis tubing (MWCO: 1000 Da) and immersed in 10 mL of DI water at

37 °C. After 1, 3, 6, 12, and 24 h, the dialysis medium was collected and replaced with fresh DI water. Concentration of cabazitaxel in the medium was analyzed using HPLC.

2.9 Cellular Uptake of the Micelle

PSMA-positive prostate cancer C4–2 cells were used in the cellular uptake study. Briefly, 2×10^5 C4–2 cells were seeded in 24-well plates 24 h before the study. The cells were then incubated with DUPA-coupled micelle, micelle without DUPA, and cabazitaxel at 37°C for 0.5 and 1 h. After the incubation, the cells were washed with PBS and lysed with RIPA buffer. A portion of the lysate is aliquot for BCA assay, and the remaining lysate was mixed with 4N NaOH and incubated at room temperature for 1 h. Phosphate buffer was added to neutralize the solution, followed by the addition of DCM (200 μL) and incubation for 5 min to extract the drug. After centrifugation using a microcentrifuge, the supernatant DCM layer was collected, evaporated at room temperature, and reconstituted with acetonitrile for the analysis of cabazitaxel using HPLC. The HPLC system was equipped with a Shimadzu LC-20AT pump, a SIL-10AF autosampler and a SPD-10A UV detector. The BCA protein assay kit (Pierce, Rockford, IL) was used to quantitate the total protein concentration in the cell lysate. Cellular uptake was normalized to the total protein content of the samples.[24]

2.10 Penetration and Uptake Study in a 3-D Tumor Spheroid Model

3-D tumor spheroids of C4–2 cells were prepared as we described before.[29, 47, 48] Briefly, 6×10^3C4–2 cells were suspended in 100 μL Spheroid Formation ECM and then seeded in a Corning™ 96-well ultra-low attachment microplate. The plate was centrifuged at 300 g for 15 min at 4°C, followed by incubation at 37°C to form the spheroids.

Coumarin-6, a hydrophobic dye, was used to mimic cabazitaxel in the uptake and penetration studies. Coumarin-6-loaded micelles with or without DUPA modification were added to the wells and incubated at 37°C for 2 h. After washing with PBS, the spheroids were collected and fixed using 10% formalin. For the cellular uptake study, the fixed spheroids were analyzed under a fluorescence microscope (LEICA DMI3000B). To evaluate the tumor penetration efficiency of the micelles, the fixed spheroids were examined using a confocal microscope (Leica TCS SP5, Germany) as described.[29, 48]

2.11 Cell Cytotoxicity

Cellular cytotoxicity of the micelles and free cabazitaxel were evaluated in C4–2 cells. The cells were plated in 96-well plates at a density of 5×10^3 cells/well 24 h before the assay. The cells were then incubated with cabazitaxel-loaded micelles and free cabazitaxel at 37°C for 0.5, 1 and 24 h, followed by replacement with fresh medium. An MTT assay was conducted to determine cellular cytotoxicity.

2.12 *In Vivo* Anti-Tumor Activity

Anti-tumor activity study was conducted according to the animal protocol approved by the Institutional Animal Care and Use Committee (IACUC) at the University of Missouri-Kansas City. Male nude mice were housed in a temperature-controlled room with a 12 h light-dark cycle. One million C4–2 cells were mixed with matrigel at a ratio 1:1 (v/v) and subcutaneously implanted into the right flank of the nude mice. The tumors were allowed to

grow to a mean volume of 100 mm^3 before the mice were randomly assigned into four groups for the treatment with saline, free cabazitaxel, cabazitaxel-loaded micelle coupled with DUPA, and cabazitaxel-loaded micelle. The formulations were administered via the tail vein at 5mg/kg every three days. Tumor volume was monitored on a daily basis and calculated according to the equation: tumor volume = (length × $width^2$)/2.

Tumor sections were stained with hematoxylin and eosin (H&E), and apoptosis in tumor specimen were evaluated using the Click-iT Plus TUNEL Assay Kit (Invitrogen, CA) as previously described.[29]

2.13 Statistical analysis

Statistical analysis was performed using a two-way analysis of variance (ANOVA) with Tukey's post hoc test. $P<0.05$ was considered statically significant.

3. Results and Discussion

Despite the tremendous success of immunotherapy in various cancers, chemotherapy is still the mainstay for advanced prostate cancer. Cabazitaxel is a promising second-generation taxane for the treatment of docetaxel-resistant cancers. It was approved as the second line of treatment for metastatic castration-resistant prostate cancer. However, its low water solubility and poor specificity lead to high systemic toxicity, which limits its therapeutic applications. In this study, we developed a targeted polymeric micelle to encapsulate cabazitaxel to increase its solubility and tumor uptake (Figure 1).

The amphiphilic polymer is biocompatible and composed of PEG_{2000} as the hydrophilic segment and cholesterol as the hydrophobic core. PEG_{2000} not only facilitates micelle formation but also forms the outer shell to prolong the systemic circulation time of the micelle. To minimize the "PEG dilemma" effect on cellular uptake of the micelle,[49] we incorporated an MMP2-responsive linker (PLGVRK) in the amphiphilic polymer (cholesterol-PLGVRK-PEG_{2000}) to dissociate the micelle in the tumor microenvironment, thus enhancing the cellular uptake of cabazitaxel. A fraction of the amphiphilic polymers (cholesterol-PEG_{3000}-DUPA) were coupled with the PSMA-specific ligand DUPA to achieve targeted delivery of the micelle to prostate cancer. PEG_{3000} rather than PEG_{2000} was used in DUPA-coupled polymers to guarantee the exposure of DUPA on the surface of the micelles.

3.1 Synthesis of Cholesterol-PLGVRK-PEG

Cholesterol-PLGVRK-PEG_{2000} (4) was synthesized by conjugating PEG_{2000}-NHS to cholesterol-PLGVRK-NH_2(Figure 2B). The final product was purified by HPLC using a Waters C18 column (250 mm × 4.6 mm, 5 μm) at a flow rate of 1.0 mL/min. The mobile phase consisted of water and acetonitrile with a linear gradient increasing from 0% to 90% acetonitrile over 35 min. The chemical structure of cholesterol-PLGVRK-PEG_{2000} was confirmed with ^1H NMR. As shown in Figure 2D, the large multiple peaks at δ 3.4–3.7 ppm (a) correspond to the protons of methylene groups in PEG, which has repeating ethylene glycol units, the peaks present at δ 0.6 to 1.2 ppm (b) represent the protons in cholesterol, and the peaks at approximately δ 1–2.6, 3–3.4, 3.7–5.5, and 6.5–7.7 ppm (c) represent

several protons in the peptide PLGVRK. The presence of peaks corresponding to PEG along with cholesterol and peptide collectively, confirms that cholesterol-PLGVRK-PEG_{2000} was successfully conjugated. Cholesterol-PEG_{3000}-DUPA was synthesized as illustrated in Figure 2C, and its NMR spectrum was presented in Figure 2D. The presence of the characteristic peaks of PEG at δ 3.4–3.7 ppm (a) along with peaks at approximately δ 2.0 ppm (d) (represent the methylene moiety of the glutamate group in DUPA), and the peak at approximately δ 7.2 ppm (e) (represents the amide of the uredo group in DUPA) confirms the successful conjugation of cholesterol-PEG_{3000}-DUPA. Additionally, the peak at approximately 2.5 ppm (s) represents the DMSO solvent. The repeating units of ethylene glycol in PEG give overwhelming signals and subduing other signals.

3.2 Preparation and Characterization of the Cabazitaxel-Loaded Polymeric Micelles

The cabazitaxel-loaded polymeric micelle was prepared using the solvent evaporation method as described.[29]Non-targeted polymeric micelles were prepared using cholesterol-PLGVRK-PEG_{2000} alone, while cholesterol-PLGVRK-PEG_{2000} and cholesterol-PEG_{3000}-DUPA were mixed at a 9:1 molar ratio in the preparation of the DUPA-coupled micelles. The cabazitaxel-loaded micelle is clear and transparent, indicating a well-dispersed and stable formulation.

The average particle size of DUPA-coupled micelles was 196 nm with a PDI of 0.13, suggesting a uniform dispersity of the micelles (Figure 3A). Zeta potential of the micelle is approximately 0.56mV (Figure3B). TEM images revealed spherical and homogeneous micelles with an average particle size of approximately 200 nm (Fig 3C), which is consistent with the results from DLS.

The CMC of the micelle was determined using iodine as a probe. As illustrated in Figure 3D, the CMC is approximately 5.7μg/mL, which is more than 11 times lower than the blood concentration of the micelle in mice after systemic injection at a dose of 5 mg/Kg. As a result, the micell is expected to be stable in the blood of mice.

Drug loading capacity and encapsulation efficiency are fundamental physicochemical characteristics of polymeric micelles. As shown in Figure 3E and 3F, the micellar formulation efficiently loaded cabazitaxel at different drug/polymer ratios. The highest drug loading was 23.33 % at the drug/polymer ratio of 1:0.5 (w/w), with an entrapment efficiency of 70%. By contrast, the highest entrapment efficiency was 79.69%at the drug-polymerratio of 1:0.25 (w/w), with a drug loading of 10.88%. The micelle solutions were clear and did not show any signs of aggregation or turbidity at all drug/polymer ratios, indicating excellent stability of the micelles.

3.3 MMP-2-ResponsiveDrug Release

We incorporated an MMP-2-responsive peptide between cholesterol and PEG to minimize the “PEG dilemma” effect on cellular uptake and specifically release cabazitaxel in the tumor microenvironment. MMP2 belongs to the family of matrix metalloproteinases whose function is to degrade the extracellular matrix and basement membrane. As a result, these enzymes play an important role in tumor growth and metastasis.[50] MMP-2 is

overexpressed in many types of cancers including prostate cancer.[31–33] PLGVRK is an MMP-2-responsive peptide that has been used in tumor-targeted delivery systems.[51–55]

According to our hypothesis, the MMP-2-responsive linker PLGVRK in the micelle will be cleaved by MMP-2 present in the prostate tumor microenvironment, leading to the dissociation of the micelle structure and release of encapsulated cabazitaxel in the tumor microenvironment to exert its activity. We first evaluated the stability of the linker itself in PBS buffer containing recombinant human MMP-2 protein. As shown in Figure 4A, the MMP-2-responsive substrate is stable for up to 6 h in the absence of MMP-2 but efficiently cleaved in the presence of MMP-2 (10 ng/μL) with a half-life of 4 h.

We next examined drug release profile of the micelle (5 μM) in the presence of MMP-2. As illustrated in Figure 4B, in the presence of 200 ng/mL MMP-2, the micelle released cabazitaxel steadily, and approximately 80 % of the drug was released within 24 h. By contrast, in the absence of MMP-2, only about 10% of the drug is released after 24 h. These results demonstrated the MMP-2-responsive drug release of the micelle.

3.4 Cellular Uptake Study in Monolayers of Prostate Cancer cells

Although nanocarriers are believed to passively accumulate in tumors by the enhanced permeability and retention (EPR) effect, the hypothesis has been challenged by a number of groups. For example, Chan et al. demonstrated that majority of nanoparticles enter tumors via an active process through endothelial cells in the tumor microenvironment.[56] The result clearly highlighted the importance of active targeting in cancer therapy using nanomedicine. Attachment of tumor-specific ligands to drug-loaded nanocarriersis the most efficient way to achieve active targeting in cancer therapy.[3] In this study, we chose PSMA as a molecular target because it is the most prominent and validated biomarker in prostate cancer. PSMA is overexpressed at exceptionally high levels in prostate cancer cells, and its expression level increases as the disease progresses.[24, 57, 58] PSMA is a transmembrane protein that possesses an internalization or transportation capability, making it an ideal target for the delivery of anti-cancer therapeutics.[9, 59] Several types of PSMA-specific ligands, such as antibodies, peptides and small molecular agents, have been identified and utilized in prostate cancer therapy and imaging. We selected the recently identified PSMA-specific ligand DUPA, which is a urea-based small molecular compound with a very high affinity (Kd 14 nM) to PSMA.[60] Very recently, DUPA was adopted as the targeting ligand in a radio-ligand therapy, which demonstrated promising effects in clinical trials.[61, 62]

We evaluated whether the incorporation of DUPA as a PSMA-targeting ligand enhances the delivery of the micelle to prostate cancer cells (Figure 5). The polymeric micelles and free cabazitaxel were incubated with PSMA-positive prostate cancer C4–2 cells for 0.5 and 1 h. As shown in Figure 5, the micelle coupled with DUPA exhibited the highest uptake, while free drug showed the lowest uptake. Compared with free cabazitaxel, the micelle coupled with DUPA exhibited nearly three- and five-fold higher uptake after 0.5 and 1 h incubation, respectively. The micelle coupled with DUPA also exhibited approximately 1.5- and 2.1-fold higher uptake than unmodified micelle after 0.5 and 1 h incubation, respectively. The results clearly demonstrated that coupling of the PSMA-specific ligand DUPA to the micelle

significantly enhanced the cellular uptake of its cargo by PSMA-positive prostate cancer cells.

3.5 Cellular Uptake and Penetration of the Micelle in 3-D Tumor Spheroids

We further studied the cellular uptake of the micelle in a 3-D spheroid tumor model, which mimics the physiological characteristics of solid tumors. As illustrated in Figure 6A and 6B, the micelle coupled with DUPA exhibited nearly three-fold and two-fold higher fluorescent intensity compared with free dye and unmodified micelle, respectively.

Limited tumor penetration is one of the major hurdles for cancer therapeutics. We, therefore, examined the tumor penetration efficiency of the PSMA-targeted micellar delivery system in 3-D tumor spheroids (Figure 6C and 6D). After two hours of incubation, the micelle coupled with DUPA showed the deepest penetration into the tumor spheroids, suggesting that the PSMA-specific ligand enhances the penetration of the carrier to the tumor microenvironment.

3.6 Cytotoxicity Study

Having demonstrated high cellular uptake and tumor penetration of the micelle coupled with DUPA, we sought to evaluate the *in vitro* cytotoxicity of the micelle in prostate cancer C4–2 cells. The cells were incubated with 5 μM cabazitaxel and equivalent concentration of cabazitaxel-loaded micelle for 0.5, 1, and 24 h. As illustrated in Figure7, the blank micelle does not exhibit any cytotoxicity in the cells after 24 h incubation, indicating good safety of the carrier. The micelle coupled with DUPA exhibited significantly higher cytotoxicity than free cabazitaxel at both 0.5 and 1 h incubation times, suggest that the micelle can efficiently deliver the drug into the cells. This is in accordance with the cellular uptake results (Figure 5). However, the micelle showed similar cytotoxicity as free drug after 24 h incubations. This is because free drug can also efficiently diffuse into the cells *in vitro* after long incubation period.

3.7 *In Vivo* Anti-Tumor Activity Study

Anti-tumor activity of the micelle was examined in nude male mice implanted with C4–2 cells. Approximately 1×10^7 C4–2 cells were subcutaneously implanted into the right flank of each mouse. Once the tumor volume reached $100mm^3$, the mice were randomly divided into four groups for the treatment. Cabazitaxel and micelles were intravenously injected via the tail vein at a dose of 5 mg cabazitaxel/kg every three days. The selection of the dose is based on previous reports of cabazitaxel in animal studies.[63–65] As illustrated in Figure8 (A–C), after three injections on days 2, 5 and 8, the micelle coupled with DUPA showed the highest efficacy in inhibiting tumor growth compared to other groups. Unmodified micelle showed slightly better effect compared to free cabazitaxel, but the difference is not statistically significant (p-value of 0.13).

A TUNEL assay of the tumor specimen revealed that the micelle coupled with DUPA induced significantly higher apoptosis compared to other groups (Figure 8D and 8E). The number of apoptotic cells in the DUPA-coupled micelle group were approximately 4 and 8 times higher compared to the unmodified micelle group and free cabazitaxel group,

respectively (Figure8E). Moreover, The TUNEL assay result was consistent with the H&E staining results (Figure 8D). Together, these results indicate that the micelle coupled with DUPA exhibited the best anti-cancer activity *in vivo*. Our findings also highlight the importance of active targeting in prostate cancer targeted therapy.

4. Conclusion

In this study, an enzyme-responsive, PSMA-targeting, and cabazitaxel-loaded micellar drug delivery system was developed, characterized and evaluated in prostate cancer cells. The polymeric micelle is biocompatible with a high drug loading efficiency. The micelle shows MMP-2-responsive release of the encapsulated drug. Compared to the micelle without DUPA modification, the DUPA-coupled micelle demonstrates higher cellular uptake in monolayers of prostate cancer cells and higher tumor penetration in 3-D tumor spheroids. Moreover, the DUPA-coupled micelle showed the highest anti-tumor activity in mice bearing xenograft tumors. Our results demonstrate the importance of active targeting in targeted prostate cancer therapy. Encapsulating cabazitaxel in the micelle increases its activity and is expected to reduce its dose and systemic toxicity, which is a major hurdle in its clinical applications. Moreover, the polymeric micelle may server as a promising nanoscale platform for the targeted delivery of other chemotherapeutic agents to prostate cancer.

Acknowledgements

This work was supported by the National Institutes of Health (1R01GM121798 and 1R01CA231099). Kun Cheng, PhD was also supported by an American Cancer Society-Lee National Denim Day Research Scholar Grant (RSG-15-132-01-CDD). This work was supported in part by funds provided from the University of Missouri-Kansas City School of Graduate Studies Research Grant program.

References

[1]. Siegel RL, Miller KD, Jemal A, Cancer statistics, 2018, CA: a cancer journal for clinicians 68(1) (2018) 7–30. [PubMed: 29313949]

[2]. Ghosh D, Peng X, Leal J, Mohanty R, Peptides as drug delivery vehicles across biological barriers, Journal of pharmaceutical investigation 48(1) (2018) 89–111. [PubMed: 29963321]

[3]. Barve A, Jin W, Cheng K, Prostate cancer relevant antigens and enzymes for targeted drug delivery, Journal of controlled release : official journal of the Controlled Release Society 187 (2014) 118–32.

[4]. Oudard S, TROPIC: Phase III trial of cabazitaxel for the treatment of metastatic castration-resistant prostate cancer, Future oncology 7(4) (2011) 497–506. [PubMed: 21463139]

[5]. Paller CJ, Antonarakis ES, Cabazitaxel: a novel second-line treatment for metastatic castration-resistant prostate cancer, Drug design, development and therapy 5 (2011) 117–24.

[6]. de Bono JS, Oudard S, Ozguroglu M, Hansen S, Machiels JP, Kocak I, Gravis G, Bodrogi I, Mackenzie MJ, Shen L, Roessner M, Gupta S, Sartor AO, Investigators T, Prednisone plus cabazitaxel or mitoxantrone for metastatic castration-resistant prostate cancer progressing after docetaxel treatment: a randomised open-label trial, Lancet 376(9747) (2010) 1147–54. [PubMed: 20888992]

[7]. Kommineni N, Mahira S, Domb AJ, Khan W, Cabazitaxel-Loaded Nanocarriers for Cancer Therapy with Reduced Side Effects, Pharmaceutics 11(3) (2019).

[8]. Aydin O, Youssef I, Yuksel Durmaz Y, Tiruchinapally G, ElSayed ME, Formulation of Acid-Sensitive Micelles for Delivery of Cabazitaxel into Prostate Cancer Cells, Molecular pharmaceutics 13(4) (2016) 1413–29. [PubMed: 26977718]

[9]. Ghosh A, Heston WD, Tumor target prostate specific membrane antigen (PSMA) and its regulation in prostate cancer, Journal of cellular biochemistry 91(3) (2004) 528–39. [PubMed: 14755683]

[10]. Ross JS, Sheehan CE, Fisher HA, Kaufman RP Jr., Kaur P, Gray K, Webb I, Gray GS, Mosher R, Kallakury BV, Correlation of primary tumor prostate-specific membrane antigen expression with disease recurrence in prostate cancer, Clin Cancer Res 9(17) (2003) 6357–62. [PubMed: 14695135]

[11]. Jin W, Barve A, Cheng K, PSMA-Specific Ligands in Prostate Cancer Diagnosis and Therapy, European Medical Journal Urology 4(1) (2016) 62–69.

[12]. Kularatne SA, Venkatesh C, Santhapuram HK, Wang K, Vaitilingam B, Henne WA, Low PS, Synthesis and biological analysis of prostate-specific membrane antigen-targeted anticancer prodrugs, Journal of medicinal chemistry 53(21) (2010) 7767–77. [PubMed: 20936874]

[13]. Kuroda K, Liu H, Kim S, Guo M, Navarro V, Bander NH, Saporin toxin-conjugated monoclonal antibody targeting prostate-specific membrane antigen has potent anticancer activity, The Prostate 70(12) (2010) 1286–94. [PubMed: 20623630]

[14]. Aggarwal S, Singh P, Topaloglu O, Isaacs JT, Denmeade SR, A dimeric peptide that binds selectively to prostate-specific membrane antigen and inhibits its enzymatic activity, Cancer research 66(18) (2006) 9171–7. [PubMed: 16982760]

[15]. Wolf P, Gierschner D, Buhler P, Wetterauer U, Elsasser-Beile U, A recombinant PSMA-specific single-chain immunotoxin has potent and selective toxicity against prostate cancer cells, Cancer immunology, immunotherapy : CII 55(11) (2006) 1367–73. [PubMed: 16547705]

[16]. Thomas TP, Patri AK, Myc A, Myaing MT, Ye JY, Norris TB, Baker JR Jr., In vitro targeting of synthesized antibody-conjugated dendrimer nanoparticles, Biomacromolecules 5(6) (2004) 2269–74. [PubMed: 15530041]

[17]. Jin W, Qin B, Chen Z, Liu H, Barve A, Cheng K, Discovery of PSMA-specific peptide ligands for targeted drug delivery, Int J Pharm 513(1–2) (2016) 138–147. [PubMed: 27582001]

[18]. Bandari RP, Jiang Z, Reynolds TS, Bernskoetter NE, Szczodroski AF, Bassuner KJ, Kirkpatrick DL, Rold TL, Sieckman GL, Hoffman TJ, Connors JP, Smith CJ, Synthesis and biological evaluation of copper-64 radiolabeled [DUPA-6-Ahx-(NODAGA)-5-Ava-BBN(7–14)NH2], a novel bivalent targeting vector having affinity for two distinct biomarkers (GRPr/PSMA) of prostate cancer, Nuclear medicine and biology 41(4) (2014) 355–63. [PubMed: 24508213]

[19]. Kularatne SA, Wang K, Santhapuram HK, Low PS, Prostate-specific membrane antigen targeted imaging and therapy of prostate cancer using a PSMA inhibitor as a homing ligand, Molecular pharmaceutics 6(3) (2009) 780–9. [PubMed: 19361233]

[20]. Roy J, Nguyen TX, Kanduluru AK, Venkatesh C, Lv W, Reddy PV, Low PS, Cushman M, DUPA conjugation of a cytotoxic indenoisoquinoline topoisomerase I inhibitor for selective prostate cancer cell targeting, Journal of medicinal chemistry 58(7) (2015) 3094–103. [PubMed: 25822623]

[21]. Rahbar K, Ahmadzadehfar H, Kratochwil C, Haberkorn U, Schafers M, Essler M, Baum RP, Kulkarni HR, Schmidt M, Drzezga A, Bartenstein P, Pfestroff A, Luster M, Lutzen U, Marx M, Prasad V, Brenner W, Heinzel A, Mottaghy FM, Ruf J, Meyer PT, Heuschkel M, Eveslage M, Bogemann M, Fendler WP, Krause BJ, German Multicenter Study Investigating 177Lu-PSMA-617 Radioligand Therapy in Advanced Prostate Cancer Patients, Journal of nuclear medicine : official publication, Society of Nuclear Medicine 58(1) (2017) 85–90.

[22]. Alshememry AK, El-Tokhy SS, Unsworth LD, Using properties of tumor microenvironments for controlling local, on-demand delivery from biopolymer-based nanocarriers, Current pharmaceutical design (2017).

[23]. Du J, Lane LA, Nie S, Stimuli-responsive nanoparticles for targeting the tumor microenvironment, Journal of controlled release : official journal of the Controlled Release Society 219 (2015) 205–214.

[24]. Barve A, Jain A, Liu H, Jin W, Cheng K, An enzyme-responsive conjugate improves the delivery of a PI3K inhibitor to prostate cancer, Nanomedicine : nanotechnology, biology, and medicine 12(8) (2016) 2373–2381.

[25]. Tai W, Shukla RS, Qin B, Li B, Cheng K, Development of a peptide-drug conjugate for prostate cancer therapy, Molecular pharmaceutics 8(3) (2011) 901–12. [PubMed: 21510670]

[26]. Ke W, Zha Z, Mukerabigwi JF, Chen W, Wang Y, He C, Ge Z, Matrix Metalloproteinase-Responsive Multifunctional Peptide-Linked Amphiphilic Block Copolymers for Intelligent Systemic Anticancer Drug Delivery, Bioconjugate chemistry 28(8) (2017) 2190–2198. [PubMed: 28661654]

[27]. Nguyen MM, Carlini AS, Chien MP, Sonnenberg S, Luo C, Braden RL, Osborn KG, Li Y, Gianneschi NC, Christman KL, Enzyme-Responsive Nanoparticles for Targeted Accumulation and Prolonged Retention in Heart Tissue after Myocardial Infarction, Advanced materials 27(37) (2015) 5547–52. [PubMed: 26305446]

[28]. Wang HX, Yang XZ, Sun CY, Mao CQ, Zhu YH, Wang J, Matrix metalloproteinase 2-responsive micelle for siRNA delivery, Biomaterials 35(26) (2014) 7622–34. [PubMed: 24929619]

[29]. Li Y, Zhao Z, Liu H, Fetse JP, Jain A, Lin CY, Cheng K, Development of a Tumor-Responsive Nanopolyplex Targeting Pancreatic Cancer Cells and Stroma, ACS Appl Mater Interfaces 11(49) (2019) 45390–45403. [PubMed: 31769963]

[30]. Zhu L, Kate P, Torchilin VP, Matrix metalloprotease 2-responsive multifunctional liposomal nanocarrier for enhanced tumor targeting, ACS Nano 6(4) (2012) 3491–8. [PubMed: 22409425]

[31]. Trudel D, Fradet Y, Meyer F, Harel F, Tetu B, Significance of MMP-2 expression in prostate cancer: an immunohistochemical study, Cancer research 63(23) (2003) 8511–5. [PubMed: 14679018]

[32]. Stearns M, Stearns ME, Evidence for increased activated metalloproteinase 2 (MMP-2a) expression associated with human prostate cancer progression, Oncology research 8(2) (1996) 69–75. [PubMed: 8859777]

[33]. Pajouh MS, Nagle RB, Breathnach R, Finch JS, Brawer MK, Bowden GT, Expression of metalloproteinase genes in human prostate cancer, Journal of cancer research and clinical oncology 117(2) (1991) 144–50. [PubMed: 1848860]

[34]. Kularatne SA, Zhou Z, Yang J, Post CB, Low PS, Design, synthesis, and preclinical evaluation of prostate-specific membrane antigen targeted (99m)Tc-radioimaging agents, Molecular pharmaceutics 6(3) (2009) 790–800. [PubMed: 19361232]

[35]. Kozikowski AP, Nan F, Conti P, Zhang J, Ramadan E, Bzdega T, Wroblewska B, Neale JH, Pshenichkin S, Wroblewski JT, Design of remarkably simple, yet potent urea-based inhibitors of glutamate carboxypeptidase II (NAALADase), Journal of medicinal chemistry 44(3) (2001) 298–301. [PubMed: 11462970]

[36]. Sengupta P, Basu S, Soni S, Pandey A, Roy B, Oh MS, Chin KT, Paraskar AS, Sarangi S, Connor Y, Sabbisetti VS, Kopparam J, Kulkarni A, Muto K, Amarasiriwardena C, Jayawardene I, Lupoli N, Dinulescu DM, Bonventre JV, Mashelkar RA, Sengupta S, Cholesterol-tethered platinum II-based supramolecular nanoparticle increases antitumor efficacy and reduces nephrotoxicity, Proceedings of the National Academy of Sciences of the United States of America 109(28) (2012) 11294–9. [PubMed: 22733767]

[37]. Zhang J, Garrison JC, Poluektova LY, Bronich TK, Osna NA, Liver-targeted antiviral peptide nanocomplexes as potential anti-HCV therapeutics, Biomaterials 70 (2015) 37–47. [PubMed: 26298393]

[38]. Suh W, Han SO, Yu L, Kim SW, An angiogenic, endothelial-cell-targeted polymeric gene carrier, Molecular therapy : the journal of the American Society of Gene Therapy 6(5) (2002) 664–72. [PubMed: 12409265]

[39]. Hermanson GT, Bioconjugate Techniques, Second Edition, Academic Press; 2 edition (5 2, 2008).

[40]. Krishnamurthy VM, Semetey V, Bracher PJ, Shen N, Whitesides GM, Dependence of effective molarity on linker length for an intramolecular protein-ligand system, Journal of the American Chemical Society 129(5) (2007) 1312–20. [PubMed: 17263415]

[41]. Zhang H, Liu X, Wu F, Qin F, Feng P, Xu T, Li X, Yang L, A Novel Prostate-Specific Membrane-Antigen (PSMA) Targeted Micelle-Encapsulating Wogonin Inhibits Prostate Cancer Cell Proliferation via Inducing Intrinsic Apoptotic Pathway, International journal of molecular sciences 17(5) (2016).

[42]. Wu F, Xu T, Liu C, Chen C, Song X, Zheng Y, He G, Glycyrrhetinic acid-poly(ethylene glycol)-glycyrrhetinic acid tri-block conjugates based self-assembled micelles for hepatic targeted delivery of poorly water soluble drug, TheScientificWorldJournal 2013 (2013) 913654.

[43]. Cholkar K, Hariharan S, Gunda S, Mitra AK, Optimization of dexamethasone mixed nanomicellar formulation, AAPS PharmSciTech 15(6) (2014) 1454–67. [PubMed: 24980081]

[44]. Wei Z, Hao J, Yuan S, Li Y, Juan W, Sha X, Fang X, Paclitaxel-loaded Pluronic P123/F127 mixed polymeric micelles: formulation, optimization and in vitro characterization, Int J Pharm 376(1–2) (2009) 176–85. [PubMed: 19409463]

[45]. Hait SK, Moulik SP, Determination of critical micelle concentration (CMC) of nonionic surfactants by donor-acceptor interaction with lodine and correlation of CMC with hydrophile-lipophile balance and other parameters of the surfactants, Journal of Surfactants and Detergents 4(3) (2001) 303–309.

[46]. Yu Y, He Y, Xu B, He Z, Zhang Y, Chen Y, Yang Y, Xie Y, Zheng Y, He G, He J, Song X, Self-assembled methoxy poly(ethylene glycol)-cholesterol micelles for hydrophobic drug delivery, Journal of pharmaceutical sciences 102(3) (2013) 1054–62. [PubMed: 23280512]

[47]. Zhao Z, Li Y, Shukla R, Liu H, Jain A, Barve A, Cheng K, Development of a Biocompatible Copolymer Nanocomplex to Deliver VEGF siRNA for Triple Negative Breast Cancer, Theranostics 9(15) (2019) 4508–4524. [PubMed: 31285776]

[48]. Liu H, Zhao Z, Zhang L, Li Y, Jain A, Barve A, Jin W, Liu Y, Fetse J, Cheng K, Discovery of low-molecular weight anti-PD-L1 peptides for cancer immunotherapy, J Immunother Cancer 7(1) (2019) 270. [PubMed: 31640814]

[49]. Hatakeyama H, Akita H, Harashima H, A multifunctional envelope type nano device (MEND) for gene delivery to tumours based on the EPR effect: a strategy for overcoming the PEG dilemma, Advanced drug delivery reviews 63(3) (2011) 152–60. [PubMed: 20840859]

[50]. Ozden F, Saygin C, Uzunaslan D, Onal B, Durak H, Aki H, Expression of MMP-1, MMP-9 and TIMP-2 in prostate carcinoma and their influence on prognosis and survival, Journal of cancer research and clinical oncology 139(8) (2013) 1373–82. [PubMed: 23708302]

[51]. Lei Q, Qiu WX, Hu JJ, Cao PX, Zhu CH, Cheng H, Zhang XZ, Multifunctional Mesoporous Silica Nanoparticles with Thermal-Responsive Gatekeeper for NIR Light-Triggered Chemo/Photothermal-Therapy, Small 12(31) (2016) 4286–98. [PubMed: 27376247]

[52]. Zhang J, Yuan ZF, Wang Y, Chen WH, Luo GF, Cheng SX, Zhuo RX, Zhang XZ, Multifunctional envelope-type mesoporous silica nanoparticles for tumor-triggered targeting drug delivery, Journal of the American Chemical Society 135(13) (2013) 5068–73. [PubMed: 23464924]

[53]. Huang CW, Li Z, Conti PS, Radioactive smart probe for potential corrected matrix metalloproteinase imaging, Bioconjugate chemistry 23(11) (2012) 2159–67. [PubMed: 23025637]

[54]. Wang Y, Shen P, Li C, Wang Y, Liu Z, Upconversion fluorescence resonance energy transfer based biosensor for ultrasensitive detection of matrix metalloproteinase-2 in blood, Analytical chemistry 84(3) (2012) 1466–73. [PubMed: 22242647]

[55]. Lee S, Cha EJ, Park K, Lee SY, Hong JK, Sun IC, Kim SY, Choi K, Kwon IC, Kim K, Ahn CH, A near-infrared-fluorescence-quenched gold-nanoparticle imaging probe for in vivo drug screening and protease activity determination, Angewandte Chemie 47(15) (2008) 2804–7. [PubMed: 18306196]

[56]. Sindhwani S, Syed AM, Ngai J, Kingston BR, Maiorino L, Rothschild J, MacMillan P, Zhang Y, Rajesh NU, Hoang T, Wu JLY, Wilhelm S, Zilman A, Gadde S, Sulaiman A, Ouyang B, Lin Z, Wang L, Egeblad M, Chan WCW, The entry of nanoparticles into solid tumours, Nature Materials (2020).

[57]. Bostwick DG, Pacelli A, Blute M, Roche P, Murphy GP, Prostate specific membrane antigen expression in prostatic intraepithelial neoplasia and adenocarcinoma: a study of 184 cases, Cancer 82(11) (1998) 2256–61. [PubMed: 9610707]

[58]. Wright GL Jr., Haley C, Beckett ML, Schellhammer PF, Expression of prostate-specific membrane antigen in normal, benign, and malignant prostate tissues, Urologic oncology 1(1) (1995) 18–28. [PubMed: 21224086]

[59]. Elsasser-Beile U, Buhler P, Wolf P, Targeted therapies for prostate cancer against the prostate specific membrane antigen, Current drug targets 10(2) (2009) 118–25. [PubMed: 19199907]

[60]. Baur B, Solbach C, Andreolli E, Winter G, Machulla HJ, Reske SN, Synthesis, Radiolabelling and In Vitro Characterization of the Gallium-68-, Yttrium-90- and Lutetium-177-Labelled PSMA Ligand, CHX-A″-DTPA-DUPA-Pep, Pharmaceuticals 7(5) (2014) 517–29. [PubMed: 24787458]

[61]. Rasul S, Hacker M, Kretschmer-Chott E, Leisser A, Grubmuller B, Kramer G, Shariat S, Wadsak W, Mitterhauser M, Hartenbach M, Haug AR, Clinical outcome of standardized (177)Lu-PSMA-617 therapy in metastatic prostate cancer patients receiving 7400 MBq every 4 weeks, Eur J Nucl Med Mol Imaging (2019).

[62]. Jackson PA, Hofman MS, Hicks RJ, Scalzo M, Violet JA, Radiation Dosimetry in (177)Lu-PSMA-617 Therapy Using a Single Post-treatment SPECT/CT: A Novel Methodology to Generate Time- and Tissue-specific Dose Factors, Journal of nuclear medicine : official publication, Society of Nuclear Medicine (2019).

[63]. Qu N, Lee RJ, Sun Y, Cai G, Wang J, Wang M, Lu J, Meng Q, Teng L, Wang D, Teng L, Cabazitaxel-loaded human serum albumin nanoparticles as a therapeutic agent against prostate cancer, Int J Nanomedicine 11 (2016) 3451–9. [PubMed: 27555767]

[64]. Song Y, Tian Q, Huang Z, Fan D, She Z, Liu X, Cheng X, Yu B, Deng Y, Self-assembled micelles of novel amphiphilic copolymer cholesterol-coupled F68 containing cabazitaxel as a drug delivery system, Int J Nanomedicine 9 (2014) 2307–17. [PubMed: 24872693]

[65]. Vrignaud P, Semiond D, Lejeune P, Bouchard H, Calvet L, Combeau C, Riou JF, Commercon A, Lavelle F, Bissery MC, Preclinical antitumor activity of cabazitaxel, a semisynthetic taxane active in taxane-resistant tumors, Clin Cancer Res 19(11) (2013) 2973–83. [PubMed: 23589177]

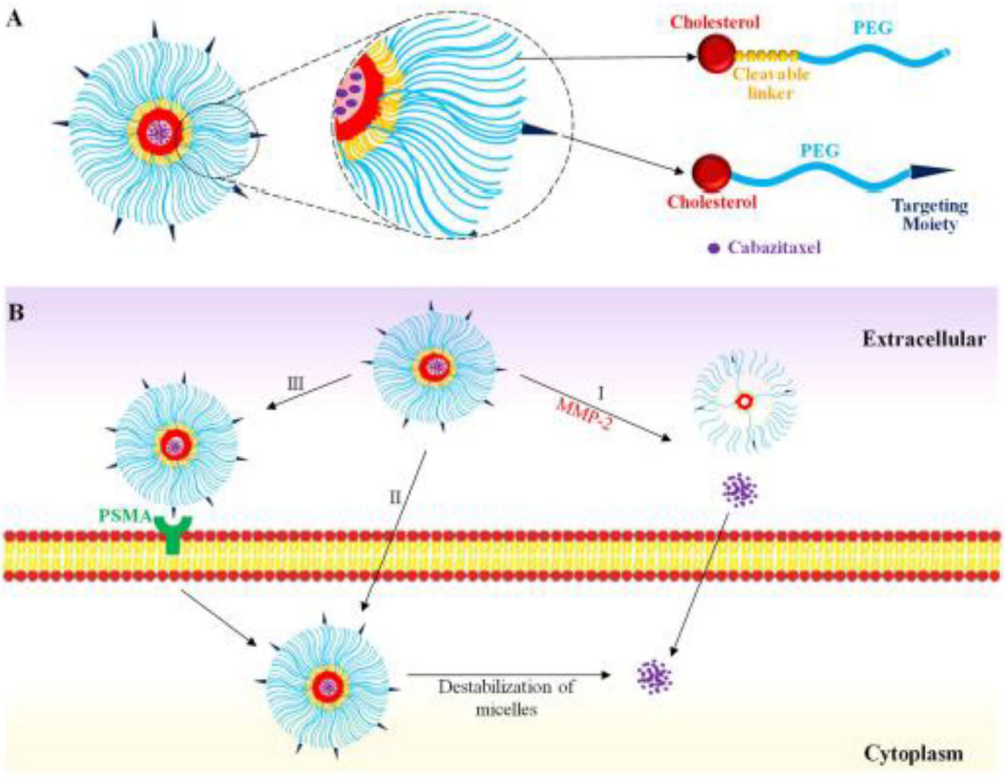

Figure 1. Schematics of the enzyme-responsive polymeric micelle.

(A) Fabrication of the polymeric micelle. (B) Delivery of the polymeric micelle to prostate cancer cells. (I) MMP-2 mediated destabilization of the micelle to release cabazitaxel; (II) Nonspecific endocytosis of the micelle; (III) PSMA-mediated endocytosis.

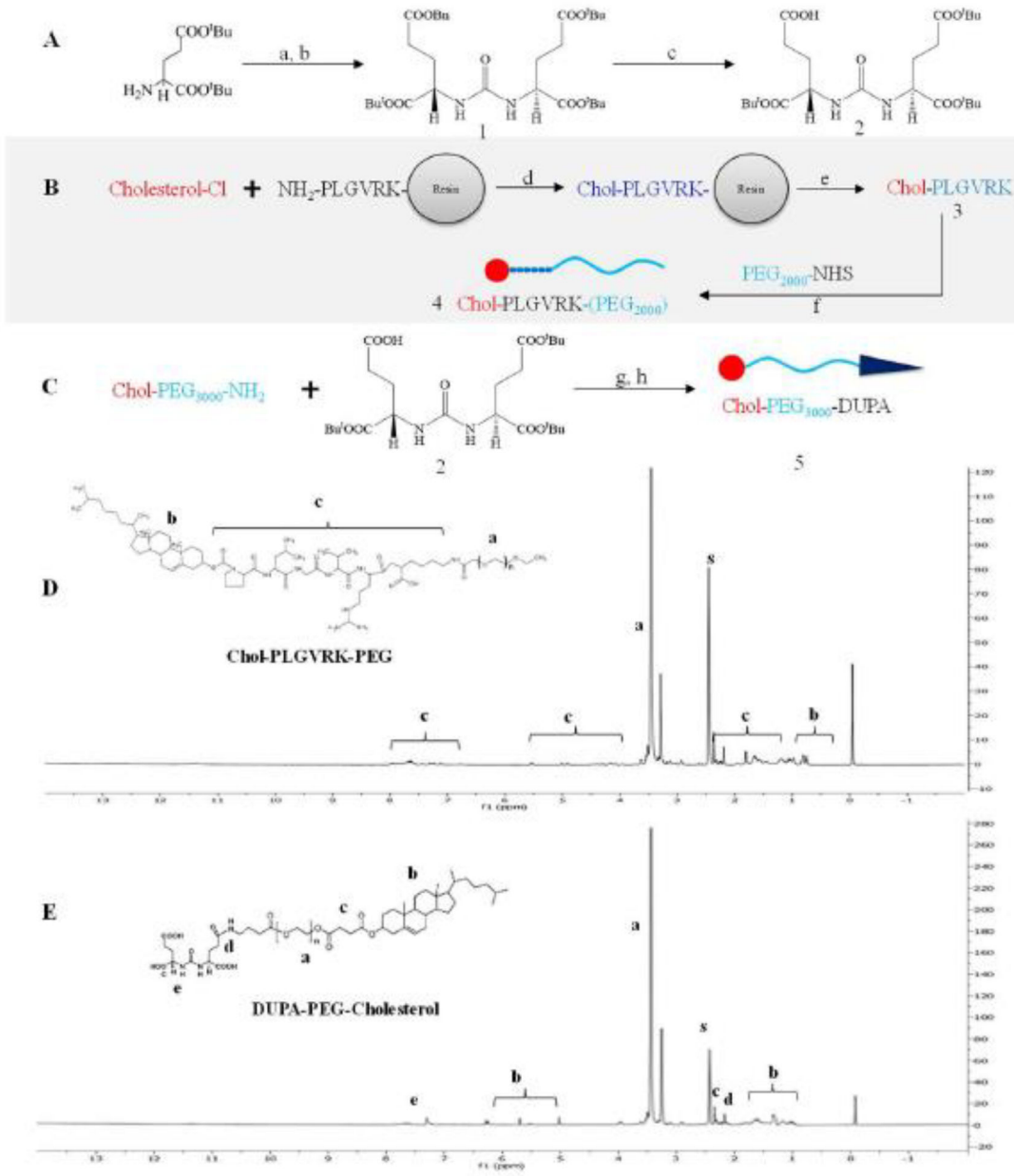

Figure 2. Synthetic scheme.

(A) Synthetic scheme of DUPA. Reagents and conditions: (a) triphosgene, TEA/DCM, −78 °C; (b) H-L-Glu(OBn)-OtBu·HCl; (c) H2; Pd-C/DCM. (B) Synthetic scheme of cholesterol-PLGVRK-PEG_{2000}. Reagents and conditions: (d) DCM, 0–5°C; (e) TFA (95%) water (2.5%), Tips (2.5%); (f) DIPEA (0.2 mmol) in anhydrous DCM. (C) Synthetic scheme of cholesterol-PLGVRK-PEG_{3000} Block-2: (g) EDC, DCM, (h) 95% TFA in DCM for 2 h at room temperature. (D) ^{1}H NMR spectrum of cholesterol-PLGVRK-PEG_{2000}. (E) 1H NMR spectra of cholesterol-PEG_{3000}-DUPA.

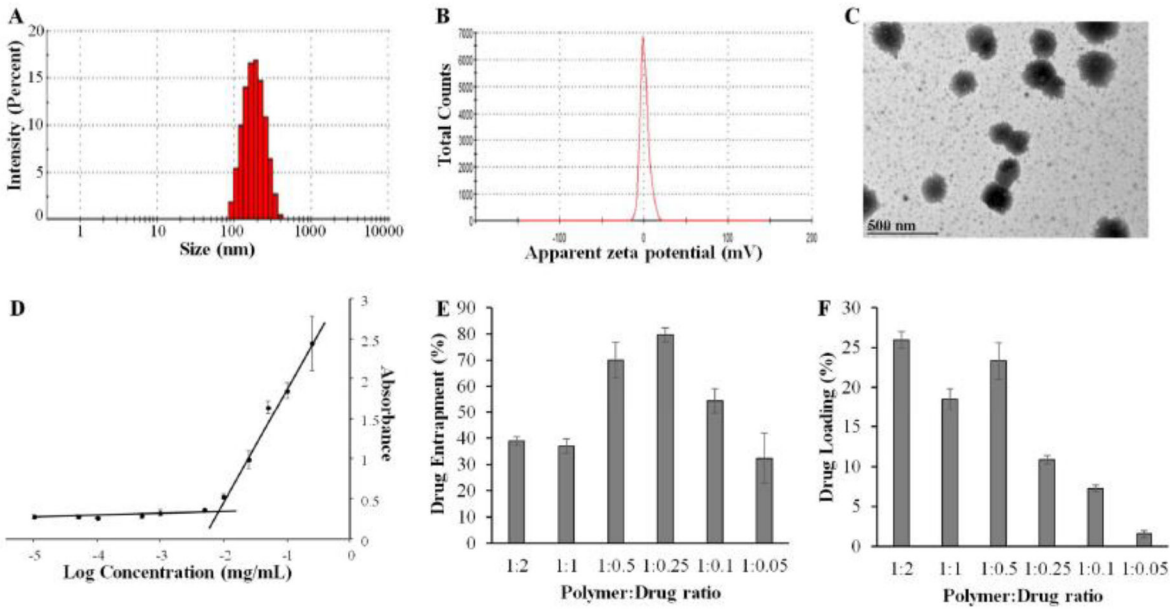

Figure 3. Characterization of cabazitaxel-loaded polymeric micelle.

(A) Size distribution. (B) Zeta potential. (C) TEM image. (D) Determination of the CMC. Drug entrapment efficiency (E) and drug loading (F) of the polymeric micelles at different polymer:drug (w/w) ratios. The results are presented as the mean ± SD (n=3).

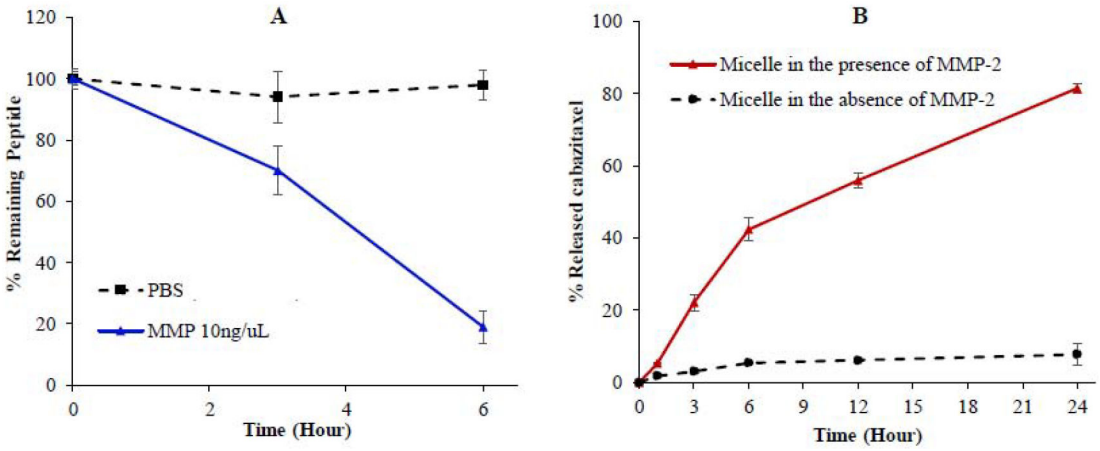

Figure 4. MMP-2-responsive drug release.

(A) Stability of the Ac-PLGVRK-NH_2 peptide in PBS and recombinant human MMP-2 protein (10 ng/μL). (B) Release of cabazitaxel from the micelle in the presence of recombinant human MMP2 (2 ng/μL). The results are presented as the mean ± SD (n = 3).

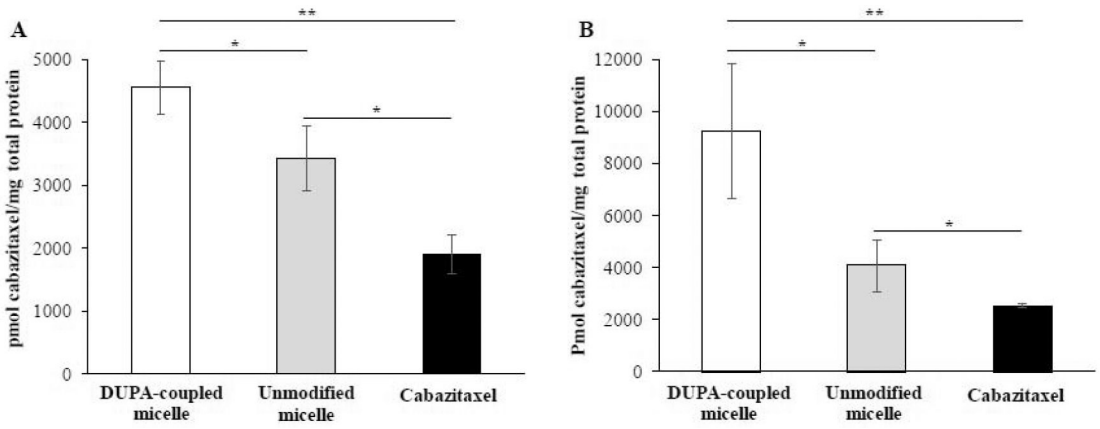

Figure 5. Cellular uptake of the micelle in C4–2 prostate cancer cells.

(A) Cellular uptake after 0.5 h incubation. (B) Cellular uptake after 1 h incubation. The results are presented as the mean ± SD (n = 3). (* $P<0.05$, ** $P<0.01$).

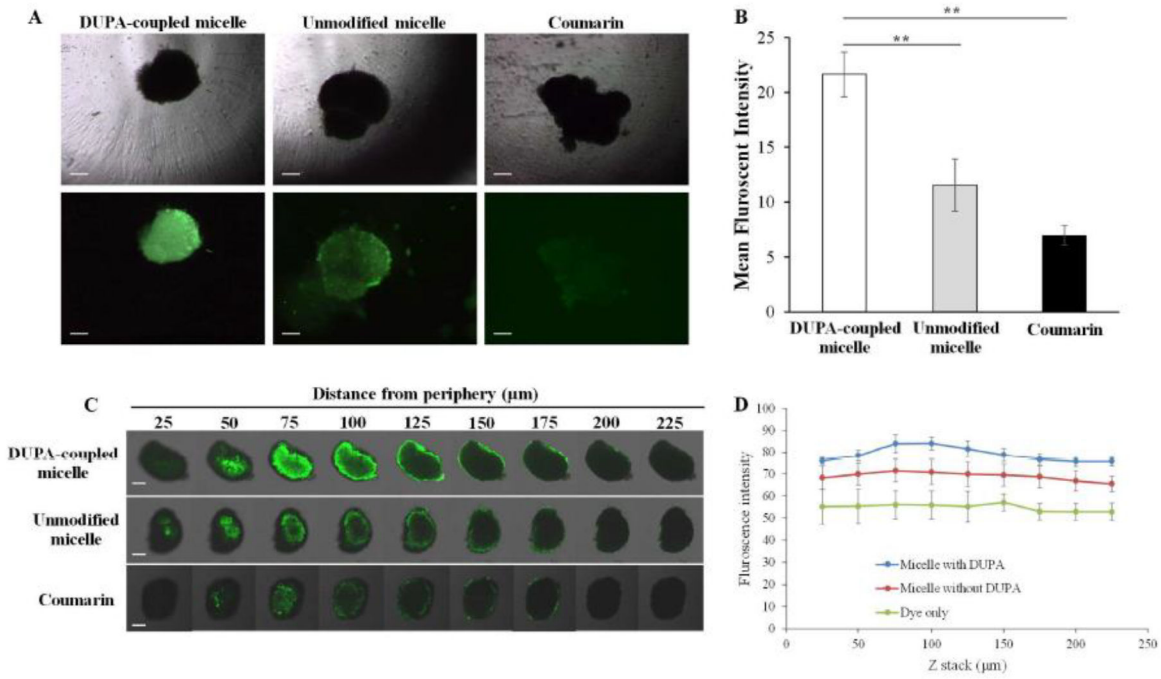

Figure 6. Cellular Uptake and Penetration of the Micelle in 3-D Tumor Spheroids

(A) Representative fluorescence images of 3-D spheroids incubated with coumarin and coumarin-loaded micelle for 2 h. Scale bar represents 200 μm. (B) Quantitative analysis of the fluorescence intensity of the spheroids. (C) Representative z-stack confocal images of 3-D spheroids incubated with coumarin and coumarin-loaded micelles for 2 h. Scale bar represents 200 μm. (D) Mean fluorescence intensity of the z-stacked confocal images vs. the distance from the periphery of the spheroids. The results are represented as the mean ± SD (n = 3). (** $P < 0.01$)

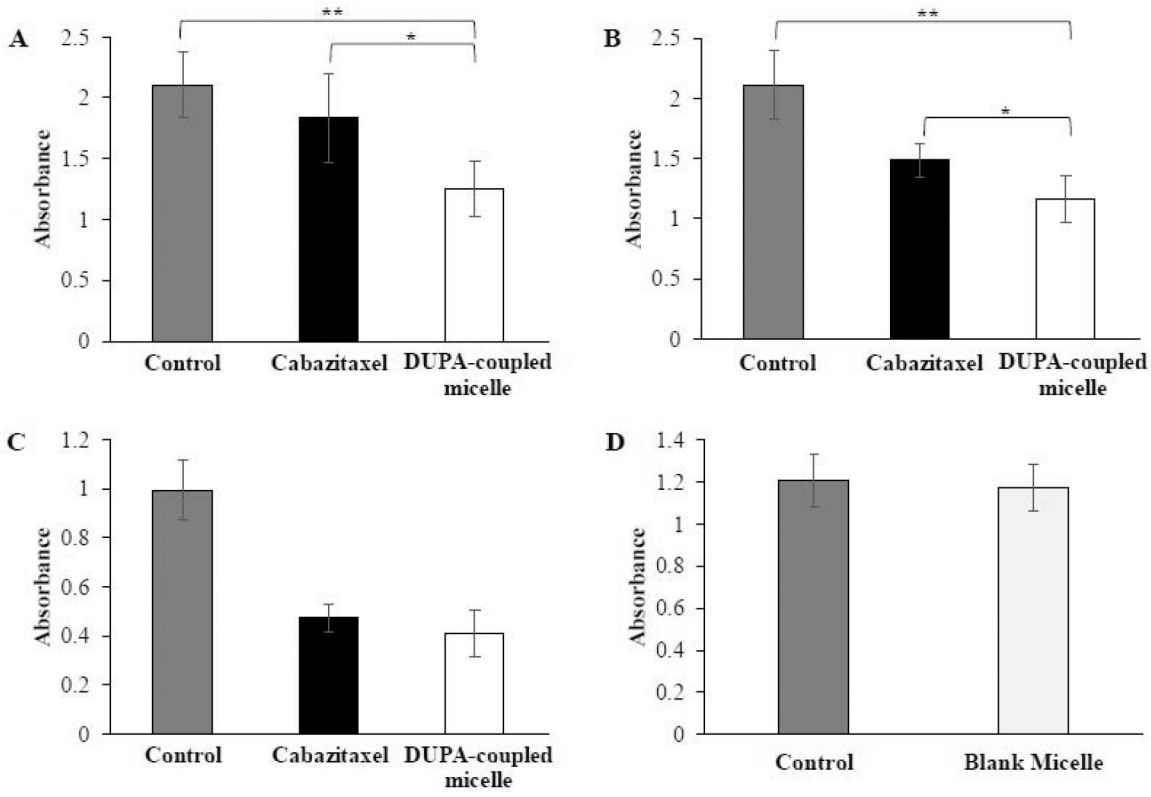

Figure 7. Cytotoxicity of the micelles in C4–2 cells.

C4–2 cells were incubated with cabazitaxel and DUPA-coupled micelle for 0.5 h (A), 1 h (B), and 24 h (C).(D) Cytotoxicity of blank micelle. The results are presented as the mean ±SD (n = 3). (* $P<0.05$, ** $P< 0.01$).

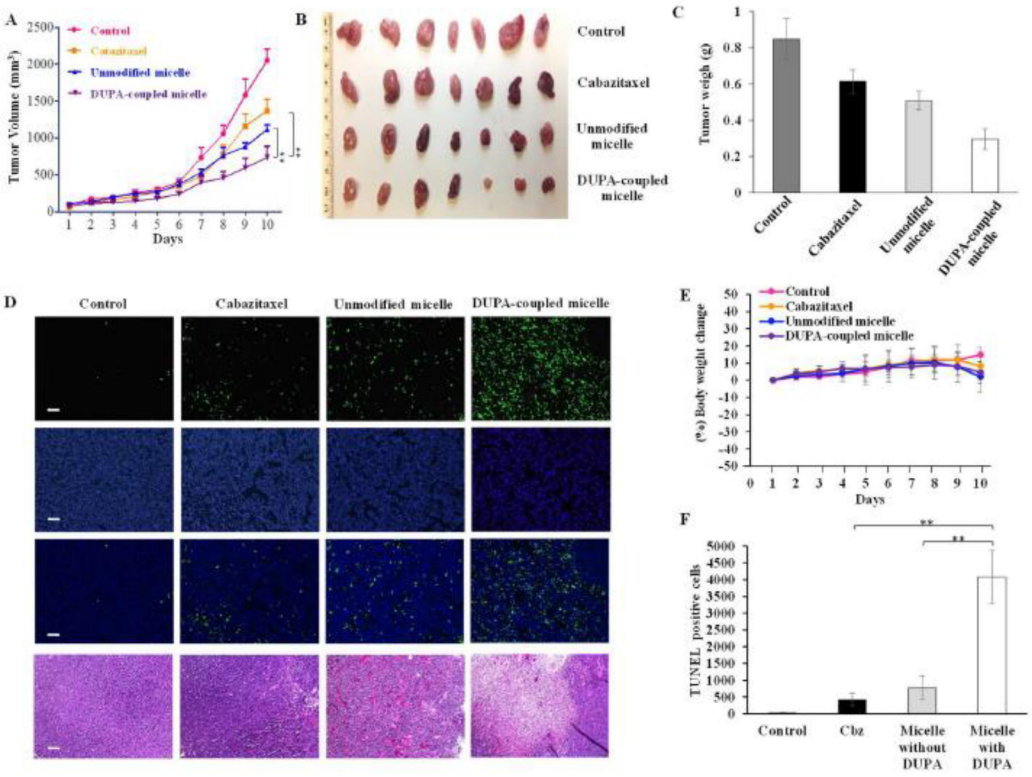

Figure 8. Anti-tumor activity of the targeted micelle in a xenograft prostate cancer mouse model.

Once the tumor volume reached 100 mm^3, the mice were randomly divided into four groups for the treatment with saline, cabazitaxel, cabazitaxel-loaded unmodified micelle, and cabazitaxel-loaded DUPA-coupled micelle. The formulations were administered at 5 mg cabazitaxel/kg via the tail vein on days 2, 5, and 8. (A) Tumor growth curves. The results are presented as the mean ± SEM (n=7). (B) Images of harvested tumors. (C) Tumor weight. The results are presented as the mean ± SEM (n = 7). (D) TUNEL assay of tumor specimen. Scale bar represents 100 μm. (E) % Body weight change, (E) Quantitative analysis of cell apoptosis in TUNEL assay. (** $P< 0.01$)